RESEARCH

Distribution, sources, and ecological risk assessment of polycyclic aromatic hydrocarbons in sediments from Baiyang Lake, China

Liguo Fu · Yaxue Sun · Hongbo Li · Yan Chen · Hui Du · Shu-xuan Liang

Abstract The issue of polycyclic aromatic hydrocarbons (PAHs) has been an environmental focus worldwide. In this study, the contents, sources, and ecological risks of sixteen PAHs in the sediment of Baiyang Lake were estimated, and a list of priority pollutants was established. The total PAH contents ranged from 114 to 1010 ng·g^{-1}. The composition of PAHs indicated that 4- to 6-ring PAHs predominated in the sediment samples. The diagnostic ratio analysis showed that combustion sources were predominant for PAHs in Baiyang Lake. Specifically, the positive matrix factorization model indicated that diesel engine emissions, gasoline engine emissions, wood combustion sources, and coal combustion sources contributed 22, 32, 24, and 22% of ∑PAHs, respectively. Based on the sediment quality guidelines, mean effects range median quotient, ecological risk quotient, and toxicity equivalent quotient methods, the comprehensive assessment results of PAHs in Baiyang Lake sediments indicated that the ecological risks were at medium and low levels. The priority pollutant list showed that benzo[b]fluoranthene and benzo[a]pyrene were the highest-priority pollutants and thus should be given more attention.

Keywords Sediments · Polycyclic aromatic hydrocarbons · Source identification · Ecological risk assessment · Priority pollutant ranking

L. Fu · Y. Sun · Y. Chen · H. Du · S. Liang
Key Laboratory of Analytical Science and Technology of Hebei Province, College of Chemistry and Materials Science, Hebei University, Baoding 071002, People's Republic of China

H. Li
Baiyangdian Basin Eco-environmental Support Center, Shijiazhuang 050056, China

S. Liang (✉)
Institute of Life Science and Green Development, Hebei University, Baoding 071002, People's Republic of China
e-mail: liangsx168@126.com

Introduction

Polycyclic aromatic hydrocarbons (PAHs) have become a worldwide environmental issue in recent decades due to their toxicity and prevalence in various environmental media (Bai et al., 2022a, b; Li et al., 2021). Some PAHs have strong teratogenic and carcinogenic effects, and exposure to these hydrocarbons can cause a variety of negative health effects (Cao et al., 2020; Li et al., 2022). Thus, the United States Environmental Protection Agency (USEPA) listed 16 of them as the main pollutants of concern in 1976 (USEPA) (Zhang et al., 2022).

PAHs are unavoidable products resulting from the incomplete combustion of carbon-containing materials; thus, they can come from natural sources

or those related to human activities. In particular, anthropogenic PAH sources have increased the contents of PAHs through either combustion (e.g., industrial pyrolysis and shipping-related and urban coal) or petrogenic sources (Han et al., 2021). Due to their hydrophobic and lipophilic properties (Corminboeuf et al., 2021), PAHs are preferentially first adsorbed onto suspended particles or deposited in surface sediments after entering aquatic environments, and sediments are considered one of their main environmental fates. The migration and transformation of PAHs in sediments have significant effects on aquatic ecology (Škrbić et al., 2018). Therefore, much attention has been given to the PAHs in sediments from different aquatic environments. PAH residues have been observed in estuarine sediments (Li et al., 2021; Montuori et al., 2016), lake sediments (Gu et al., 2017), intertidal sediments (Li et al., 2017), and bay sediments (Bateni et al., 2022; Shi et al., 2022a, b).

Source analyses of environmental pollutants are the basis for quantifying their impacts on the environment. Source-apportionment methods developed for PAHs in water environments mainly include diagnostic ratio and statistical analyses. The diagnostic ratio method directly uses the chemical properties or some chemical parameters of PAHs to identify pollution sources. To some extent, the composition of PAHs in media can reflect their main sources and input pathways. In general, 2- or 3-ring low molecular weight PAHs originate from petroleum sources, and 4- to 6-ring high molecular weight PAHs originate from combustion sources (Deng et al., 2013; Han et al., 2021; Hong et al., 2022). However, it is difficult to determine the sources and relative contribution rates of PAHs with similar compositions. Statistical analyses use mathematical means to identify sources with methods such as principal component analysis (PCA), in which multiple variables are transformed into a few comprehensive variables (Sun et al., 2022; Wang et al., 2021; Li et al., 2021; Ciucure et al., 2023). Positive matrix factorization (PMF) is one of the most widely used research methods in recent years because it uses the weighted least-squares method to perform iterative calculations and quantify the contributions of source components without measuring the source component spectrum (Gao et al., 2012; Hong et al., 2022).

To clarify whether PAHs can produce adverse effects on the ecological environment, it is necessary to assess their ecological risks. Various methods have been used to evaluate the ecological risks of PAHs in past studies, such as sediment quality guidelines (SQGs) and the quotient value method. SQGs can be used to qualitatively assess the possible ecological risk based on the contents of each PAH monomer found in the sediments, whereas the quotient value method can provide quantitative estimations based on ecotoxicity or potential carcinogenicity. The most widely used quotient value methods include the mean effects range median quotient (M-ERM-Q), ecological risk quotient (RQ), and toxicity equivalence quotient (TEQ) methods. Although all of these methods are intended to be used for risk assessments, they differ from each other in their factor-selection and assessment criteria. M-ERM-Q is used mainly to quantitatively predict the comprehensive ecotoxicity of various PAHs (Han et al., 2021; Lin et al., 2018), whereas RQ uses monomer risk standard values to estimate the ecological risks of 16 PAH monomers and $\sum_{16}$PAHs (Zhang et al., 2022). TEQ_{BaP} uses the toxicity equivalence factor (TEF) based on benzo[a] pyrene (BaP) to evaluate the carcinogenic potencies of 16 PAH monomers, thus achieving quantitative risk assessment (Ihunwo et al., 2021). These methods have been widely applied in risk assessments of PAHs in sediments. To our knowledge, however, most of the existing relevant studies have used these methods to conduct independent analyses but have failed to consider multifactor combinations.

Baiyang Lake (BYL) is the largest freshwater lake on the North China Plain. Since China announced the plan to create the Xiongan New Area, a new economic zone, special research attention has been given to the important ecological function of this lake. In the last 10 years, many people have studied the pollutants in the aquatic environment of BYL, including pollution associated with pharmaceuticals and personal products, fluorescent whitening agents, quinolone antibiotics, and perfluoroalkyl substances (Liu et al., 2019; Wu et al., 2021; Yang et al., 2021; Zhang et al., 2020). Heavy metals and microplastics are also present in lake sediments (Ji et al., 2019; Zhou et al., 2021). Previous studies only qualitatively analyzed the sources of PAHs in Baiyang Lake using the molecular diagnostic ratio method (Hu et al., 2010), while quantitatively identifying and evaluating the sources of PAHs and the contribution of each source in the study area is still unclear.

Therefore, this study aimed to (1) investigate the latest spatial distribution and composition characteristics of PAHs in the sediments covering BYL, (2) identify qualitatively and quantitatively the sources of the PAHs using the molecular diagnostic ratio (MDR) method and PMF model, (3) estimate the ecological risk of PAHs by various methods, and finally (4) rank the priority pollutants of PAH monomers according to their physicochemical properties, abundance, and ecological risk levels. This work provides a method for establishing a list of priority pollutants in sediment to promote effective water pollution control, while also providing more accurate data support for PAH pollution control in sediment of BYL.

Materials and methods

Study area and sampling

BYL, the largest freshwater, shallow lake with an herbaceous marsh wetland ecosystem in China, is located in the southeastern Xiongan New Area (39°04′–40°04′ N, 113°39′–116°11′ E). This lake

plays an important role in promoting local economic development and transportation and maintaining ecological balance (Wang et al., 2020). In the past, nine rivers flowed directly into the lake (Zhang et al., 2020). However, the monsoon climate and extensive water conservancy project construction have led to seasonal droughts and a reduction in river surface runoff (Zhao et al., 2021). Now, the Fu River is the stable replenishment stream of BYL, which mainly accepts the effluent from the upstream Baoding sewage treatment plant (Wang et al., 2014). There are 89 villages with a permanent population of approximately 279,000 around the lake. The water quality and ecosystem of the lake have been affected by domestic sewage and garbage carried by rivers and discharged by residents in the lake area, as well as by water transportation and villagers' enclosure farming activities (Yang et al., 2021).

According to the national environmental automatic monitoring points and provincial monitoring points set by China, a total of 22 sampling sites were set up in BYL (numbered as per shown in Fig. 1). In this study, all sampling was conducted in October 2021. Surface sediment (0–10 cm) was collected using a
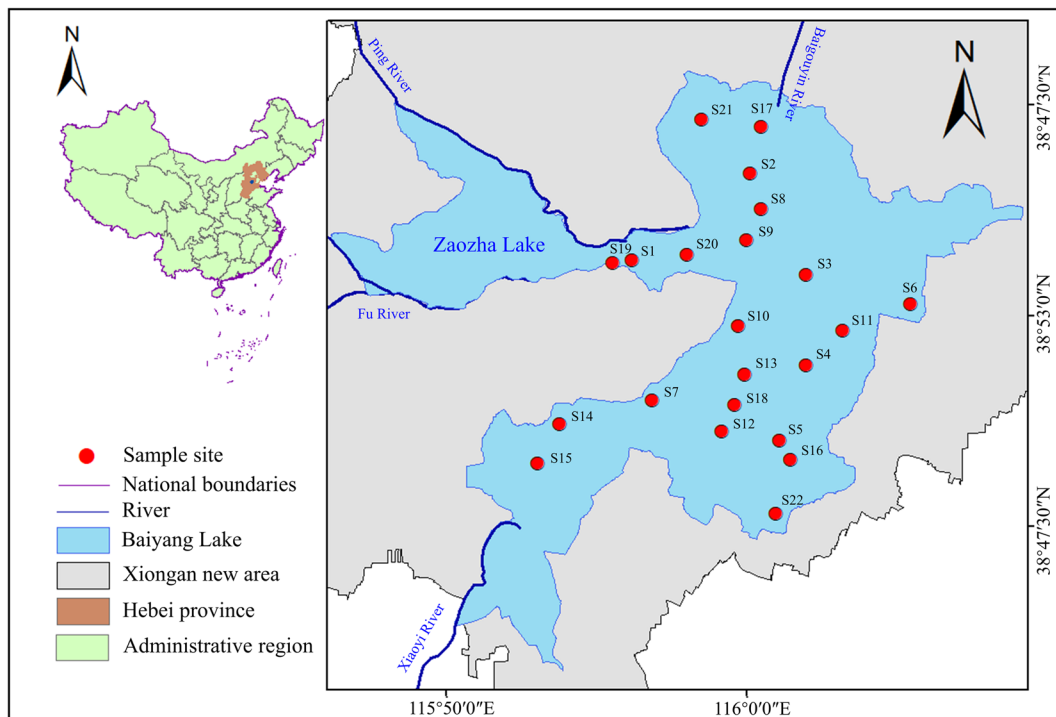
Fig. 1 Map of sampling sites in the BYL

stainless-steel grab sampler, packaged in a double-layer self-sealing bag covered with tin paper on the surface and placed into a refrigerator until being transported to the laboratory. After returning to the laboratory, the sediment samples were freeze-dried for the first time, ground with an agate mortar, poured through a 100-mesh copper sieve, and stored in a freezer until analysis.

Chemicals and materials

HPLC-grade n-hexane and dichloromethane (Tianjin, China) were used for the sample extraction and purification procedures. Analytical pure anhydrous sodium sulfate purchased from Kermel (Tianjin, China) and copper flakes purchased from Sinopharm were used for dewatering and removing sulfur in the extraction process, respectively. Neutral silica gel columns, purchased from Agilent (CA, USA), were activated with ultra-pure water. The sixteen PAH standards were purchased from Alta (Tianjin, China).

PAH extraction and analysis

All samples were extracted by ultrasonication. Briefly, 5 g of the samples was accurately weighed and mixed with anhydrous Na_2SO_4, and extracted for 0.5 h with 30 mL of n-hexane/dichloromethane (1:1, V/V) and 0.5 g copper powder. The extract was incubated for 0.5 h, and then the supernatants were transferred into a conical flask. The extraction was repeated 3 times. Subsequently, the extract was purified by neutral silica gel columns and eluted with 20 mL of dichloromethane/n-hexane (4:6, V/V) three times. The eluent was mixed, rotated, and evaporated until nearly dry, and then 10 mL of n-hexane concentrated to 1 mL was added for replacement. The final solution was filtered through a 0.22-μm filter membrane before next analysis.

Sixteen PAHs were identified using an Agilent 7890-5977A gas chromatography-mass spectrometer (GC–MS) (CA, USA). The oven temperature was set from an initial temperature of 50 °C for 2 min, ramped to 250 °C at a rate of 20 °C·min^{-1}, held for 2 min, increased to 290 °C at 5 °C·min^{-1}, and held for 5 min. Ultra-pure helium was used as the carrier gas for analysis at a flow rate of 1 mL·min^{-1} with an HP-5 fused silica capillary column (15.0 m × 0.25 mm × 0.25 μm) (Folsom, CA). Selected ion monitoring (SIM) mode was applied for analysis, and the electron bombardment energy was 70 eV. The temperatures of the sample inlet and ion source were set to 290 °C and 270 °C, respectively.

Quality assurance/quality control (QA/QC)

The tinfoil paper was soaked in dichloromethane for 24 h in advance and then dried until sampling to avoid contamination by impurities affecting the experimental analysis results. The accuracy of the standard curve was ensured before each test using the PAH standard mixture. A procedural blank was set after every 5 samples. The external standard method was used for the quantitative analysis and blank analysis to calculate the limit of detection (LOD) and limit of quantification (LOQ). Through repeated analysis, the LODs were set at 3 times the signal-to-noise ratio. In the sediment samples, the LODs and LOQs ranged from 0.10 to 0.45 ng·g^{-1} and from 0.04 to 0.18 ng·g^{-1}, respectively. The recovery of each sample was determined to be between 71 and 115%. The relative standard deviation (RSD) of the repeated test sample was low (< 10%). The $\sum_{16}$PAH contents were measured based on dry weight and were not corrected for surrogate recoveries.

Source identification of PAHs

The PMF model uses the weighted least-squares iterative calculation method to quantify the contribution rate of each major source (Ma et al., 2020). The model used in this study was EPA PMF5.0. The principle is shown in Eq. (1) as follows:

$$X_{ij} = \sum_{k=1}^{p} G_{ik}F_{kj} - E_{ij} \tag{1}$$

where X_{ij} is the content of the jth PAH compound of the ith sample, p is the number of factors, G_{ik} is the contribution of factor k to sample i, F_{kj} is the content of species j in factor profile k, and E_{ij} is the residue of the jth PAH in sample i.

The minimizing objective function Q sums all sample residuals and their uncertainties to obtain each contribution and composition of factors and then obtain the optimal solution. The Q value is obtained using following equations as Eq. (2) (Huang et al., 2021; Riaz et al., 2019):

$$Q = \sum_{i=1}^{n} \sum_{k=1}^{m} \left[\frac{E_{ij} - \sum_{k=1}^{p} G_{ij}F_{ij}}{U_{ij}} \right] \tag{2}$$

where n is the number of samples and m is the number of chemical components.

The PMF needs to be imported into the uncertainty data before running. If the PAH contents were below the method detection limit (MDL), U_{ij} was equal to the MDL; otherwise, U_{ij} was calculated using Eq. (3) as follows:

$$U_{ij} = \sqrt{\left(RSD \times X_{ij}\right)^2 + (0.5 \times MDL)^2} \tag{3}$$

where X_{ij} is the measurement matrix of species j in sample i and RSD is the relative standard deviation of the PAH content.

Ecological risk assessments

Sediment quality guidelines (SQGs)

MacDonald et al. (1996) optimized the weight of evidence of SQGs and proposed the effects range low (ERL) and effects range median (ERM). The SQGs are used to determine three concentration ranges of chemicals by comparing the contents of target pollutants with the ERL or ERM values (Li et al., 2021). When the PAH content is lower than the ERL value, effects on the biological system rarely occur. When the PAH content is between the ERL and ERM values, adverse biological effects occasionally occur. Once the PAH content in the sediment exceeds the ERM value, adverse biological effects may frequently occur (Cui et al., 2022; Han et al., 2021).

Mean effects range median quotient (M-ERM-Q)

The risk level was classified for the sediments at each sampling site of the M-ERM-Q model (Lin et al., 2018). This method is usually used to estimate the ecological risk level of PAH mixtures in sediments. The calculation model is expressed with Eq. (4) as follows:

$$M - ERM - Q = \frac{1}{n} \sum_{i=1}^{n} \frac{C_i}{ERM_i} \tag{4}$$

where C_i is the content of PAH i in sediments, ERM_i is the ERM of the corresponding PAH i, and n is the number of PAHs. The ERM data of the PAHs are shown in Table S1.

Ecological risk quotient (RQ)

The RQ was summarized by Kalf et al. (1996), who used the values of negligible contents (NCs) and maximum permissible contents (MPCs) to obtain the reference contents of 16 kinds of PAHs. The ecological risk of PAHs in sediments was evaluated by calculating risk entropy. The calculation method of the RQ is provided with Eq. (5) and Eq. (6) as follows:

$$RQ_{(NCs)} = C_{PAHs}/NC_S \tag{5}$$

$$RQ_{(MPCs)} = C_{PAHs}/MPC_S \tag{6}$$

where C_{PAHs} is the content of PAHs and $C_{QV(NCs)}$, $C_{QV(MPCs)}$, NC_S, and MPC_S are the lowest and the highest risk standard and quotient values, respectively. The specific ecological risk classifications of individual PAHs and $\sum$PAHs are listed in Table S2.

Toxicity equivalent quotient (TEQ$_{BaP}$)

The TEQ through potential toxicity was used to estimate the potential ecological risk of PAHs. The TEQ was calculated using Eq. (7) (Li et al., 2015):

$$TotalTEQ = \sum C_i \times TEF_i \tag{7}$$

where C_i is the content of PAH i in the sediment and TEF_i is the toxicity equivalent factor of compound i. The TEF data of 16 PAH monomers are shown in Table S1.

Priority pollutant ranking

To more accurately assess the adverse effects of the target pollutants in the regional sediment on the ecological environment, the multi-index comprehensive evaluation method was used to establish a list of priority pollutants. This method sets four different types of evaluation criteria: (1) environmental exposure to pollutants; (2) persistence; (3) bioaccumulation; and (4) ecological risk (Zhao et al., 2021).

The environmental exposure of pollutants is based on the detected contents of pollutants. The persistence of pollutants is mainly measured by the

biodegradation coefficient (BioWIN). The smaller the BioWIN value, the stronger the persistence of the pollutant. In addition, the octanol water partition coefficient (Kow) is used to evaluate the bioaccumulation of pollutants. The BioWIN and Kow values of all selected pollutants were obtained from the EPA EPI Suite software. Ecological risk is based on the environmental ecological risk values of the pollutants, mainly including M-ERM-Q, RQ, and TEQ_{BaP}.

Oc, BioWIN, Kow, M-ERM-Q, RQ, and TEQ_{BaP} were divided into five grades according to the geometric progression method and then assign points according to the (2/3) cumulative rank method (USEPA) (Table S3), with a full score of 100 for each standard. In calculating the weight of importance, equal weight was given to each criterion to avoid any artificial judgment deviations. The comprehensive score of each PAH monomer was the sum of the environmental exposure, persistence, bioaccumulation, and ecological risk scores, where ecological risk is the average M-ERM-Q, RQ, and TEQ_{BaP} score.

The list of priority pollutants was generated from the highest to the lowest comprehensive score. Then, the priority pollutants were further divided into three grades according to the method of arithmetic progression, among which the compounds in the first grade were the highest priority pollutants. In the RQ assignment process of PAH monomers, if $RQ_{(MPCs)}$ < 1, only the $RQ_{(NCs)}$ score was taken; however, if $RQ_{(MPCs)}$ > 1, the average score of $RQ_{(NCs)}$ and $RQ_{(MPCs)}$ was taken.

Results and discussion

PAH content levels and compositions in sediment

PAH content levels

The detected contents of each monomer of sixteen PAHs in sediments were identified by the proposed GC-MS method. The performance of this method is listed in Table S4. The contents of PAHs detected in sediments of BYL are listed in Table 1.

The contents of $\sum_{16}$PAHs in sediments ranged from 114 to 1010 ng·g^{-1}, which were higher than the contents detected by Hu et al. (2010). The contents of detected 2-ring PAHs, 3-ring PAHs, 4-ring PAHs, 5-ring PAHs, and 6-ring PAHs ranged from 5 to 44 ng·g^{-1}, 0.01 to 46 ng·g^{-1}, 0.2 to 84 ng·g^{-1}, 0.2 to 157 ng·g^{-1}, and 3 to 173 ng·g^{-1}, respectively. The contents of 2-, 3-, 4-, 5-, and 6-ring PAHs contributed 17.3%, 6.4%, 16.9%, 26.8%, and 32.6% to the $\sum$PAHs, respectively (Fig. S1). We observed

Table 1 The contents of PAHs detected in sediments of BYL

PAH	Abbreviation	Number of aromatic rings	Content (ng·g^{-1}) ($n = 22$)		
			Minimum	Maximum	Mean
Naphthalene	NaP	2	3	44	24
Acenaphthylene	Acy	3	0.1	26	3
Acenaphthene	Ace	3	0.01	14	4
Fluorene	Flu	3	0.3	32	12
Anthracene	Ant	3	1.5	46	19
Phenanthrene	Phe	3	0.4	21	7
Fluoranthene	Fla	4	0.7	74	26
Pyrene	Pyr	4	0.3	84	25
Benzo[a]anthracene	BaA	4	1.2	50	17
Chrysene	Chr	4	0.3	80	28
Benzo[b]fluoranthene	BbF	5	21	163	62
Benzo[k]fluoranthene	BkF	5	0.	63	20
Benzo[a]pyrene	BaP	5	17	132	47
Indeno [1,2,3-c, d] pyrene	IcdP	6	3	159	44
Dibenz [a, h] anthracene	DbA	5	0.2	106	22
Benzo[g, h, i]perylene	BghiP	6	3	173	48
$\sum_{16}$PAHs	–	–	114	1010	408

that most of the sites had abundant 4-, 5-, and 6-ring PAHs, as shown in Fig. S1. This characteristic composition was similar to the levels measured in the sediments of Taihu Lake (Sun et al., 2022). The average BbF content was the highest (62 ng·g^{-1}), followed by those of BghiP (48 ng·g^{-1}), BaP (47 ng·g^{-1}), IcdP (44 ng·g^{-1}), and Chr (28 ng·g^{-1}). Such a dominant composition was close to the levels measured in the sediments from the river mouths of Kaohsiung Harbor, Taiwan (Chr, BbF, BaP, IcdP, and BghiP contents of 23, 84, 45, 48, and 46 ng·g^{-1}, respectively) (Dong et al., 2014). The high ratio of high molecular weight PAHs in sediments may have been due to the hydrophobic and lipophilic properties and bacterial degradation. High molecular weight PAHs have a higher affinity for esters and are more resistant to degradation, enabling most of them to be effectively transported to and easily accumulate in sediments (Corminboeuf et al., 2021; Škrbić et al., 2018). In contrast, low-cyclicity PAHs are found mainly in the aquatic phase due to their low octanol partition coefficient and microbial degradation reducing their enrichment in sediments (Montuori et al., 2016).

Compared to other water environments that have been studied globally (Table S5), the $\sum_{16}$PAH contents in sediments from the BYL (114–1010 ng·g^{-1}) were similar to those found in the Serbian rivers and canals (Serbia) by Škrbić et al. (2018), in the Pearl River Delta (China) by Li et al. (2021), in the Marano and Grado Lagoon (Italy) by Acquavita et al. (2014), and in the Durance River (France) by Kanzari et al. (2014). The $\sum_{16}$PAH contents measured in the present study in sediment samples were higher than those found in the Yangtze River estuary, China (Liu et al., 2020), Awassa Lake, Ethiopia (Mekonnen et al., 2015), and the Amazon estuary, Brazil (Rodrigues et al., 2019) and lower than those found in the Niger River, Assai River, and Forcados River, Nigeria (Iwegbue et al., 2021), Mitty River, India (Singare, 2015), Brisbane River, Australia (Duodu et al., 2017), and Huviorn River, France (Kanzari et al., 2014). These comparisons show that the PAH contents in the sediments in our study area were at a moderate level globally.

Spatial distribution of sediment samples

Since the RSDs of the 16 kinds of PAHs were all greater than 50%, and some were even greater than

100%, the changes in the PAH contents varied greatly among different sites. The enormous content alterations of PAHs in sediments were closely related to human activities along the river because the samples were collected at different sites (Ciucure et al., 2023). The spatial variations in PAH contents in the surface sediments of rivers and lakes were attributed mainly to human activities, including traffic emissions, fuel consumption, and untreated urban wastewater emissions (Dong et al., 2022; Ciucure et al., 2023). Based on ArcGIS 10.7 software, the inverse distance-weighting method was used to interpolate the $\sum_{16}$PAH contents at different sampling points and obtain a content contour map. The spatial pattern of $\sum_{16}$PAHs in sediments from BYL is presented in Fig. 2.

As shown in Fig. 2, the $\sum_{16}$PAH contents of BYL were high in the southeastern and western lake regions, low in the southern and northern lake regions, and highest at site S19, which was located in the Fu River estuary close to villages and the traffic trunk road. A small peak in the PAH contents was observed at site S4 (935 ng·g^{-1}), which was located east of Quantou Village at one of the main river courses in the north–south direction. This river course receives most of the water flowing from the southern direction of lake at sites such as S7, S12, and S16, with frequent water traffic. Another peak occurred at site S16 (823 ng·g^{-1}), which was adjacent to a village wharf with multiple large ships and frequent personnel activities. Several water flows converged downstream, which decreased the $\sum_{16}$PAH contents at sites S11 (125 ng·g^{-1}) and S6 (245 ng·g^{-1}) at the outlet of the BYL. Other relatively high $\sum_{16}$PAH contents were detected at sites S1, S5, S7, and S8, which were located near villages with high populations and frequent production and living activities. Sites S10, S15, S17, and S21, which were located along the edges of the lake area, far from villages and near the wide-open water surface with little human activity, had low $\sum_{16}$PAH contents. These results showed that the sediments around the Fuhe River estuary and the village were seriously polluted by PAHs, especially in areas with extensive human activities (Hu et al., 2010). PAH pollution in BYL was affected mainly by human activities.
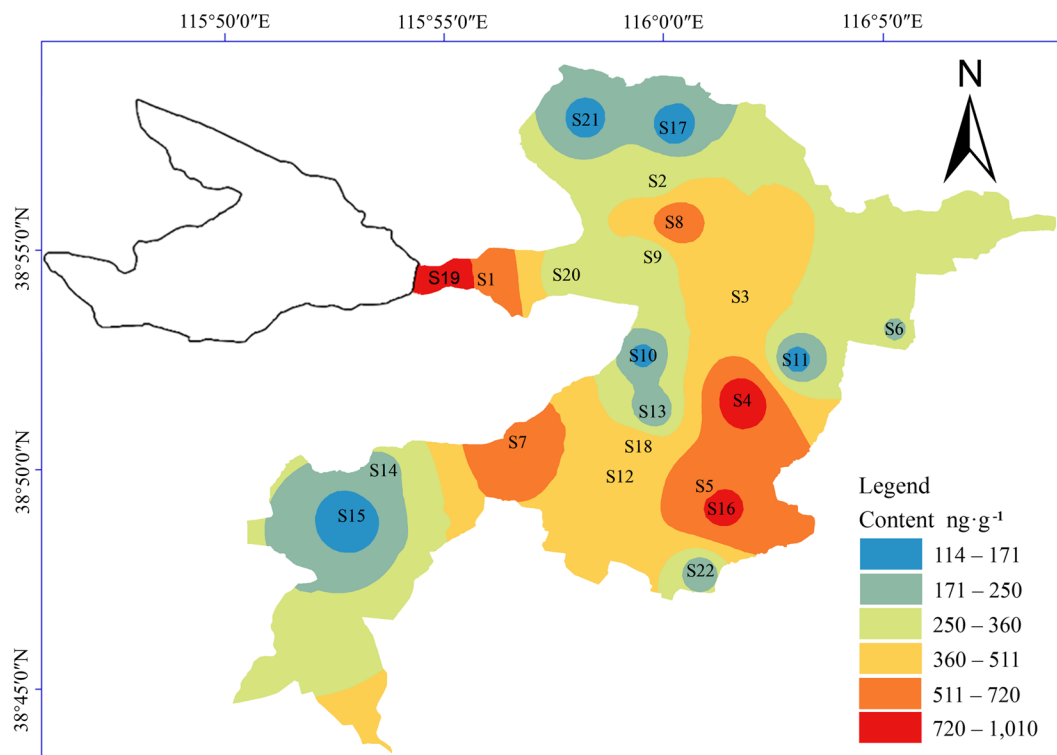
Fig. 2 Spatial distribution of $\sum_{16}$PAHs in sediments of the BYL area

Source identification of PAHs in the sediments

PAH sources identification by MDR

Different ratios of Fla/(Fla+Pyr), Ant/(Phe+Ant), IcdP/(IcdP+BghiP), and BaA/(BaA+Chr) correspond to different sources, and intuitive judgments can often be made by making ratio cross-plots (Dudhagara et al., 2016; Masood et al., 2018). Briefly, Fla/(Fla+Pyr) ratios < 0.4 indicate petroleum spills, ratios between 0.4 and 0.5 suggest petroleum combustion, and ratios > 0.5 indicate the dominance of biomass combustion. Ant/(Phe+Ant) and $\sum$LMW/$\sum$HMW values < 0.1 and > 0.1 have been determined to correspond to petroleum leakage and combustion, respectively. BaA/(BaA+Chr) ratios < 0.2, between 0.2 and 0.35, and over 0.35, as well as IcdP/(IcdP+BghiP) ratios < 0.2, between 0.2 and 0.5, or > 0.5, are attributed to petroleum spills, petroleum combustion, and biomass combustion, respectively (Han et al., 2021; Lin et al., 2018).

In this study, the Ant/(Ant+Phe) ratios at all sites (except S20) were above 0.1 (Fig. 3a), and the

fountainhead of PAHs could thus be attributed to combustion sources. The BaA/(BaA+Chr) ratios of most sampling points were greater than 0.2, indicating combustion sources, while the ratios of some points were greater than 0.35, suggesting that mixed sources, such as petroleum, liquid fossil fuel, biomass, and coal combustion, were responsible for the PAHs (Fig. 3b) (Montuori et al., 2016). Similar conclusions were reached by observing the ratio of IcdP/(IcdP+BghiP), which indicated combustion sources (Fig. 3c). Concurrently, the $\sum$LMW/$\sum$HMW ratios indicated that the PAHs at all points were sourced from pyrogenic sources (Li et al., 2017) (Fig. 3d).

The above results obtained through different MDRs were related to the specific pollution conditions in BYL. The Fu River, one of the main rivers flowing into the lake, passes through Baoding, a light industrial city, where textile mills, paper mills, agricultural areas, and the effluent from sewage plants are mixed halfway. The exhaust gas and atmospheric particles produced by factories and intensive agricultural activities also adsorb PAHs and then may be deposited to Fu River and transported into the lake (Hu
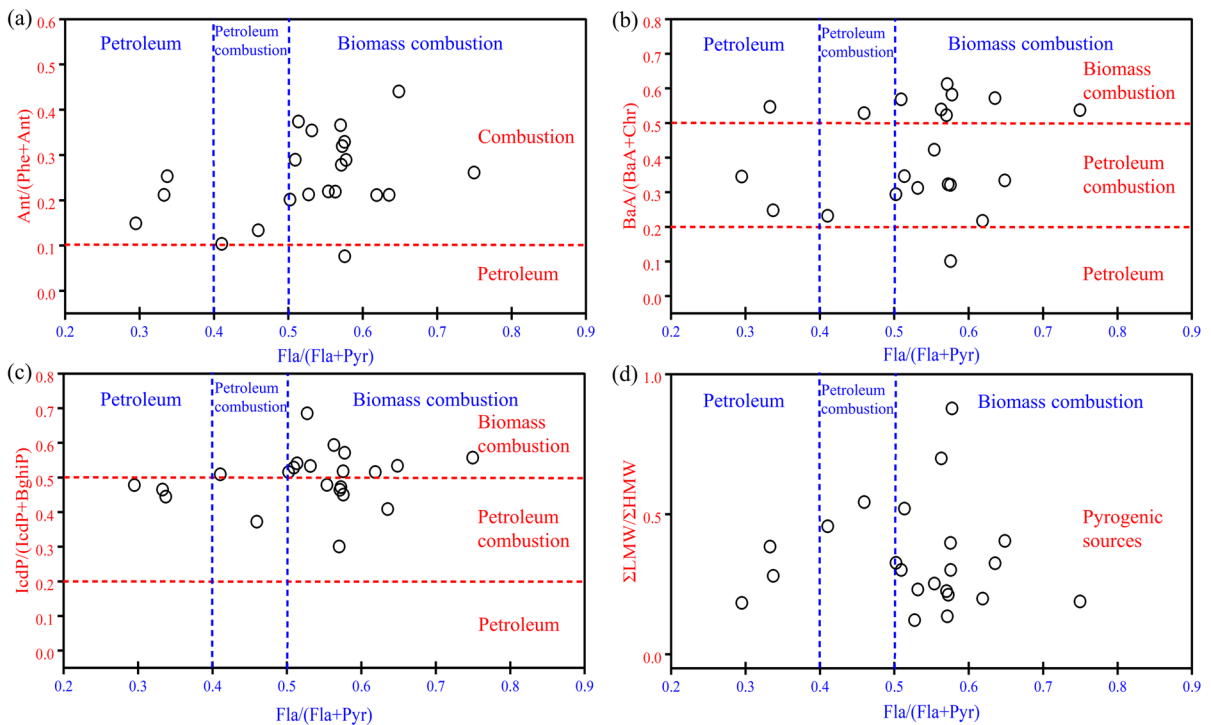
Fig. 3 PAH molecular diagnostic ratios in the sediments of BYL. **a** Ant/(Phe+Ant) versus Fla/(Fla+Pyr); **b** BaA/(BaA+Chr) versus Fla/(Fla+Pyr); **c** IcdP/(IcdP+BghiP) versus Fla/(Fla+Pyr); and **d** ∑LMW/∑HMW versus Fla/(Fla+Pyr)

et al., 2010). Therefore, the polluted water carried by the Fu River and the mixed combustion source emissions from the densely populated area of the Lake District resulted in PAH pollution caused mainly by pyrolytic sources in these areas.

PAH sources apportionment by the PMF model

To explore the possible sources of PAHs in the surface sediments of BYL, the PMF model was used to allocate the potential source according to the measured PAH contents. A dataset with 22 sampling points ×16 PAH elements was introduced to the PMF 5.0 model. By combining the possible input channels of target pollutants in the study area, four factors were finally selected to perform a quantitative analysis of the PAH sources. The Q_{robust}/Q_{true} ratio exceeded 0.98, indicating that the model was both credible and reliable (Huang et al., 2021).

The results of the PMF model are shown in Fig. 4. Factor 1 accounted for 22% of the total factor contribution and consisted mainly of BkF, IcdP, and DbA (high-cyclic PAHs). Many studies have shown that

BkF and IcdP are derived from diesel combustion (Huang et al., 2021; Li et al., 2015), and DbA is also commonly considered to be associated with transport emissions (Zheng et al., 2017). To date, many ships are still using diesel engines in BYL. Thus, factor 1 represented diesel engine emissions.

Factor 2 accounted for 32% of the total variance, and the main components were BkF and BaP, followed by Nap, Ace, DbA, and BghiP. BkF, BaP, and BghiP are markers of gasoline engine emissions (Huang et al., 2021). Nap and Ace, low cyclic weight PAHs, are generally regarded as indicators of the volatilization or leakage of oil-related products (Hu et al., 2013; Ma et al., 2020). Thus, factor 2 represented the traffic sources of gasoline engines, including land cars and small boats on water.

Factor 3 was characterized by high loadings of 3- to 4-ring PAHs and accounted for 24% of the total variance, mainly including Acy, Pyr, and Fla, followed by Ant, Flu, and Phe. Acy and Pyr are considered to be an indicator of wood and straw combustion (Shi et al., 2023; Zhang et al., 2021), and the comparatively high Fla load indicated wood combustion

Fig. 4 Factor profiles derived from the PMF models used to predict the PAH sources in the BYL sediments
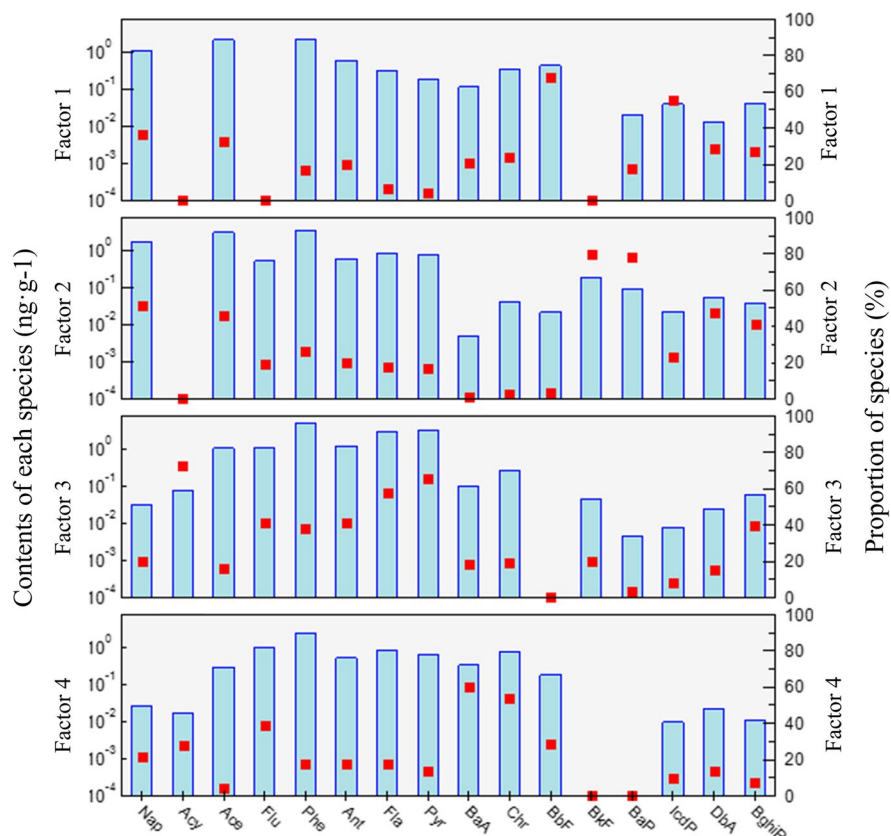
(Balgobin & Singh, 2019). Ant, Flu, and Phe are indicators of wood combustion (Zhang et al., 2021). Therefore, factor 3 represented the wood combustion source.

The main components of factor 4 were BaA, Chr, and Flu, which are the main PAHs emitted during coal combustion (Sofowote et al., 2008; Huang et al., 2023; Zhang et al., 2021). In northern rural areas, coal is widely used for household heating and cooking, so there is great consumption for household coal. Factor 4 was therefore concluded to indicate coal combustion, and accounted for 22% of the total variance.

Based on the PMF analysis results, four sources were successfully identified: (1) diesel engine emissions sources (22% of the total), (2) gasoline engine emissions (accounting for 32% of the total factor contribution), (3) wood combustion sources (accounting for 24% of the total), and (4) coal combustion sources (accounted for 22% of the total variance).

Ecological risk assessment of PAHs in the sediments

The SQG results indicated that the contents of 16 PAHs detected in all sediment samples of BYL were much lower than the ERM values (Table S1). That is, the PAHs at these points are not expected to cause serious ecological risks. Thus, the main consideration was whether the PAH monomer content at each point exceeded the ERL value. In the study area, in relation to the individual compounds, Flu had the highest frequency of contents over the corresponding ERL value (32%) and was sourced mainly from biomass combustion. The DbA level in the samples collected from Stations S16 and S19 also exceeded the ERL values, and some studies had shown that DbA was derived mainly from vehicle emissions (Zheng et al., 2017).

According to the above assessment results, PAHs produced by biomass combustion in villager production and life have potential biological toxicity effects at certain sites in lake networks, and DbA emitted from ships and vehicles may constitute a potential

ecological risk to lake sediments. In general, the ecosystem risk of PAHs in the BYL sediments is low.

As shown in Fig. 5a, in the study region, the M-ERM-Q values were lower than 0.1 in all 22 samples, showing that the comprehensive ecotoxicity of PAHs in the sediment samples of BYL was low.

The RQ was used to evaluate the ecological risk of PAHs in sediments by calculating risk entropy, and the $RQ_{(NCs)}$ and $RQ_{(MPCs)}$ values were calculated using Eqs. (5 and 6). The $RQ_{(NCs)}$ and $RQ_{(MPCs)}$ values of individual PAHs and $\sum$PAHs were calculated. The details of the $RQ_{(NCs)}$ and $RQ_{(MPCs)}$ values in sediment are listed in Table S6. The mean $RQ_{(MPCs)}$ values were < 1, while the mean $RQ_{(NCs)}$ values of PAHs (except Chr, BkF, DbA, IcdP, and BghiP) were > 1, indicating that these PAHs posed moderate ecological risks and might have certain toxicity to aquatic organisms. For the $\sum$PAH risk in BYL, the overall $RQ_{\sum PAHs(NCs)}$ values were between 1 and 800, and 41% of the samples posed moderate

risks. These results showed that the ecological risks were at moderate and low levels in BYL.

The TEQ_{BaP} values of $\sum_{16}$PAHs and $\sum_7$PAHs (BaA, Chr, BbF, BkF, BaP, IcdP, and DbA) are shown in Fig. 5b. The TEQ_{BaP} values of $\sum_{16}$PAHs were in the range of 26–220 ng·g⁻¹, with an average value of 85 ng·g⁻¹. The TEQ_{BaP} value range of $\sum_7$PAHs was 26–218 ng·g⁻¹, accounting for 98.6–99.9% of $\sum_{16}$PAHs, indicating that carcinogenic PAHs play a decisive role in the potential toxicity of the environment in this area. Among them, the BaP contents were the highest, ranging from 17 to 121 ng·g⁻¹ and accounting for 31.2–80.5% of $\sum_7$PAHs. The second was DbA, which ranged from 0.2 to 106 ng·g⁻¹, accounting for 0.6–48.5% of $\sum_7$PAHs. Some studies have shown that BaP and DbA are mostly emitted by vehicles (Huang et al., 2021; Zheng et al., 2017), so the ecological risks in the studied lake may be caused mainly by the burning of liquid fossil fuels.

Fig. 5 The M-ERM-Q values (**a**) and TEQ_{BaP} values of $\sum_{16}$PAHs and $\sum_7$PAHs (**b**)
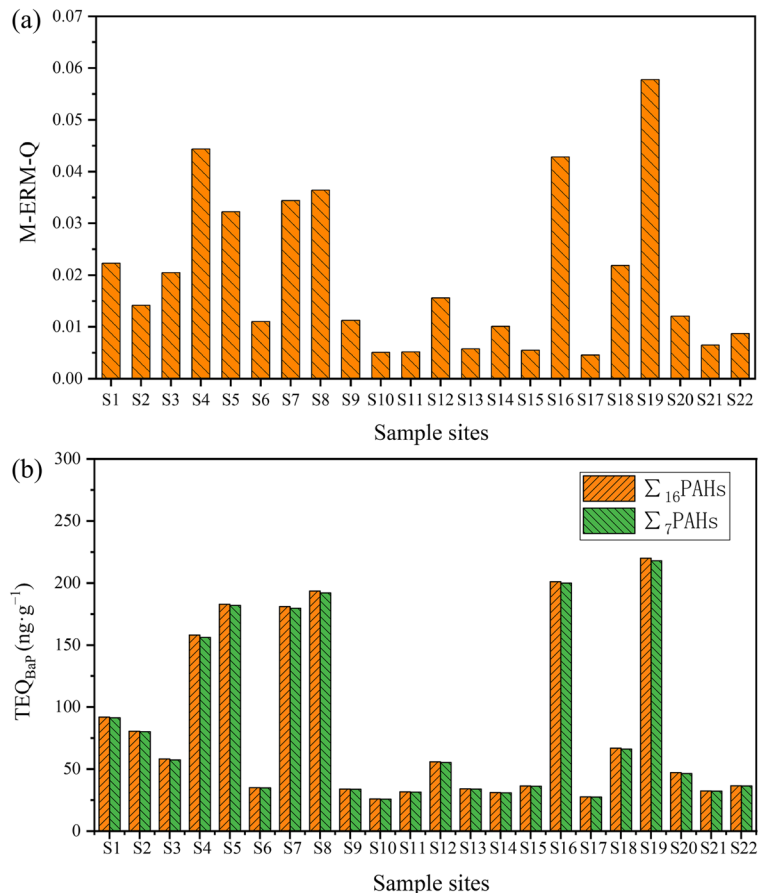
The TEQ ΣPAH values obtained in the BYL sediments were similar to those found in the sediments of the Fuxian Lake in China (83–262 ng·g^{-1}) (Gu et al., 2017). The TEQ ΣPAH values of BYL were higher than the values reported in the sediment samples from Romania Olt River dam reservoirs (0.1–106 ng·g^{-1}) (Ciucure et al., 2023), Taihu Lake in China (1–63 ng·g^{-1}) (He et al., 2023), and Wang Lake Wetland, China (1–69 ng·g^{-1}) (Shi et al., 2022a, b), but lower than the values reported in the sediment samples of the Poyang Lake, China (33–369 ng·g^{-1}) (Lu et al., 2012) and Erhai Lake, Southwest China (940–2539 ng·g^{-1}) (Huang et al., 2023).

Priority list of PAHs in BYL sediments

Different from previous research literature that only evaluated the ecological risks of PAHs in the study area (Gu et al., 2017; He et al., 2023; Hu et al., 2010; Lu et al., 2012; Shi et al., 2022a, b), priority pollutants posing serious hazards were ranked and identified from 16 PAHs in this study based on the comprehensive scoring method of multi-index parameters

(Zhao et al., 2021). All 16 PAHs were detected, and their comprehensive scores were greater than 0. The priority levels of PAHs were divided into three levels and the detailed grade allocation is listed in Table S3. Grade I PAHs included two pollutants defined as high-priority pollutants. Grade II PAHs comprised a total of 9 pollutants defined as medium-priority pollutants. Grade III contained a total of 5 substances defined as low-priority pollutants. Table 2 shows that among the 16 PAHs measured in the BYL sediments, the PAHs that should be considered for priority control were BbF and BaP, followed by DbA, BghiP, and BkF; these PAHs arise mainly from the combustion process of diesel and gasoline from traffic sources. The continuous input of these PAHs in the environment leads to the high environmental exposure level of these five PAHs, and they also have high bioaccumulation capacities and high toxicity levels. The ecological risks generated after these PAHs enter the aquatic ecosystem cannot be ignored. In the relatively late stage, the supervision and management of traffic sources (mainly ships) should be strengthened.

Table 2 Ranked results of priority PAH pollutants in BYL sediments

Number	Pollutant	Score				Total score	Risk grade
		Environmental exposure	Persistence	Bioaccumulation	Ecological risk		
1	BbF	100	100	100	77.8	377.8	I
2	BaP	100	100	100	65.4	365.4	I
3	DbA	66.7	100	100	69.6	336.3	I
4	BghiP	100	100	100	35.0	335.0	I
5	IcdP	100	100	100	25.7	325.7	I
6	BkF	66.7	100	100	28.1	294.8	I
7	Chr	66.7	100	66.7	13.4	246.7	II
8	BaA	29.6	100	66.7	47.4	243.7	II
9	Pyr	66.7	100	29.6	39.2	235.5	II
10	Fla	66.7	100	29.6	25.7	222.0	II
11	Flu	29.6	100	8.8	43.8	182.2	II
12	Nap	66.7	29.6	1.7	39.2	137.2	III
13	Phe	29.6	29.6	8.8	25.7	93.7	III
14	Ant	8.8	29.6	8.8	25.7	72.9	III
15	Acy	1.7	1.7	8.8	11.0	23.2	III
16	Ace	1.7	1.7	8.8	11.0	23.2	III

Conclusions

In this study, the pollution characteristics, sources, and ecological risk assessments of PAHs in BYL sediments were comprehensively researched. The PAH contents in the study area were at moderate levels compared to those measured globally. The proportion of high molecular weight PAHs in the sediment samples was the highest. The MDRs and PMF analysis showed that PAH pollution was mainly the result of pyrolysis sources, and the important contribution source of this pollution was mainly the combustion process of biomass and liquid fossil fuels. In addition, the contents of Flu and DbA in some places were above the corresponding ERL values and thus may occasionally cause negative ecological effects. The M-ERM-Q, RQ, and TEQ_{BaP} values of PAHs suggested that the ecological risks of PAHs at the measured sites were at low-moderate levels. The priority pollutant list showed that BbF and BaP were the highest priority pollutants, and 80.0% of 4-ring PAHs were medium-priority pollutants. This study found a slightly higher risk of PAH pollution in areas near villages and shipping lanes, which might be influenced by villagers' production and living activities, as well as by fishing boats and tourist vessels. Therefore, the local government should pay more attention to adjusting the residential energy use structure and to reasonable tourism development while maintaining systematic and continuous PAH monitoring.

Author contribution Liguo Fu: investigation, data curation, conceptualization, methodology, writing—original draft and editing. Yaxue Sun: data curation and writing—original draft. Hongbo Li: methodology, review, and project administration. Yan Chen: validation and investigation. Hui Du: investigation, data analysis, and figure drawing. Shu-xuan Liang: supervision, writing—review and editing, project administration, and funding acquisition. All authors read and approved the final manuscript.

Data availability All data supporting the findings of this study are included within this published article and its supplementary information file.

Declarations

Ethical responsibilities of authors All authors have read, have understood, and have complied as applicable with the statement "Ethical Responsibilities of Authors".

Competing interests The authors declare no competing interests.

References

Acquavita, A., Falomo, J., Predonzani, S., Tamberlich, F., Bettoso, N., & Mattassi, G. (2014). The PAH level, distribution and composition in surface sediments from a Mediterranean lagoon: The Marano and Grado Lagoon (Northern Adriatic Sea, Italy). *Marine Pollution Bulletin, 81*(1), 234–241. https://doi.org/10.1016/j.marpolbul.2014.01.041

Bai, X., Wei, J., Ren, Y., Gao, R., Chai, F., Li, H., Xu, F., & Kong, Y. (2022a). Pollution characteristics and health risk assessment of polycyclic aromatic hydrocarbons and nitrated polycyclic aromatic hydrocarbons during heating season in Beijing. *Journal of Environmental Sciences.* https://doi.org/10.1016/j.jes.2022.02.047

Bai, Y., Shi, K., Yu, H., Shang, N., Hao, W., Wang, C., Huang, T., Yang, H., & Huang, C. (2022b). Source apportionment of polycyclic aromatic hydrocarbons (PAHs) in a sediment core from Lake Dagze Co, Tibetan Plateau, China: Comparison of three receptor models. *Journal of Environmental Sciences, 121*, 224–233. https://doi.org/10.1016/j.jes.2022.01.043

Balgobin, A., & Singh, N. R. (2019). Source apportionment and seasonal cancer risk of polycyclic aromatic hydrocarbons of sediments in a multi-use coastal environment containing a Ramsar wetland, for a Caribbean island. *Science of The Total Environment, 664*, 474–486. https://doi.org/10.1016/j.scitotenv.2019.02.031

Bateni, F., Mehdinia, A., Lundin, L., & Hashtroudi, M. S. (2022). Distribution, source and ecological risk assessment of polycyclic aromatic hydrocarbons in the sediments of northern part of the Persian Gulf. *Chemosphere, 295*, 133859. https://doi.org/10.1016/j.chemosphere.2022.133859

Cao, L., Wang, D., Zhu, C., Wang, B., Cen, X., Chen, A., Zhou, H., Ye, Z., Tan, Q., Nie, X., Feng, X., Xie, Y., Yuan, J., & Chen, W. (2020). Polycyclic aromatic hydrocarbon exposure and atherosclerotic cardiovascular disease risk in urban adults: The mediating role of oxidatively damaged DNA. *Environmental Pollution, 265*(Part A), 114860. https://doi.org/10.1016/j.envpol.2020.114860

Ciucure, C., Geana, E. I., Chitescu, C., Badea, S., & Ionete, R. E. (2023). Distribution, sources and ecological risk assessment of polycyclic aromatic hydrocarbons in waters and sediments from Olt River dam reservoirs in Romania. *Chemosphere, 311*(Pt 2), 137024. https://doi.org/10.1016/j.chemosphere.2022.137024

Corminboeuf, A., Montero-Serrano, J. C., & St-Louis, R. (2021). Spatial and temporal distributions of polycyclic aromatic hydrocarbons in sediments from the Canadian Arctic Archipelago. *Marine Pollution Bulletin, 171*, 112729. https://doi.org/10.1016/j.marpolbul.2021.112729

Cui, M., Xu, S., Song, W., Ye, H., Huang, J., Liu, B., Dong, B., & Xu, Z. (2022). Trace metals, polycyclic aromatic hydrocarbons and polychlorinated biphenyls in the

surface sediments from Sanya River, China: Distribution, sources and ecological risk. *Environmental Pollution, 294*, 118614. https://doi.org/10.1016/j.envpol.2021.118614

Deng, W., Li, X. G., Li, S. Y., Ma, Y. Y., & Zhang, D. H. (2013). Source apportionment of polycyclic aromatic hydrocarbons in surface sediment of mud areas in the East China Sea using diagnostic ratios and factor analysis. *Marine Pollution Bulletin, 70*(1-2), 266–273. https://doi.org/10.1016/j.marpolbul.2013.02.032

Dong, C. D., Chen, C. F., & Chen, C. W. (2014). Vertical profile, sources, and equivalent toxicity of polycyclic aromatic hydrocarbons in sediment cores from the river mouths of Kaohsiung Harbor, Taiwan. *Marine Pollution Bulletin, 85*(2), 665–671. https://doi.org/10.1016/j.marpolbul.2013.09.037

Dong, L., Lin, L., He, J., Pan, X., Wu, X., Yang, Y., Jing, Z., Zhang, S., & Yin, G. C. (2022). PAHs in the surface water and sediments of the middle and lower reaches of the Han River, China: Occurrence, source, and probabilistic risk assessment. *Process Safety and Environmental Protection, 164*, 208–218. https://doi.org/10.1016/j.psep.2022.06.009

Dudhagara, D. R., Rajpara, R. K., Bhatt, J. K., Gosai, H. B., Sachaniya, B. K., & Dave, B. P. (2016). Distribution, sources and ecological risk assessment of PAHs in historically contaminated surface sediments at Bhavnagar coast, Gujarat, India. *Environmental Pollution, 213*, 338–346. https://doi.org/10.1016/j.envpol.2016.02.030

Duodu, G. O., Ogogo, K. N., Mummullage, S., Harden, F., Goonetilleke, A., & Ayoko, G. A. (2017). Source apportionment and risk assessment of PAHs in Brisbane River sediment, Australia. *Ecological Indicators, 73*, 784–799. https://doi.org/10.1016/j.ecolind.2016.10.038

Gao, B., Guo, H., Wang, X. M., Zhao, X. Y., Ling, Z. H., Zhang, Z., & Liu, T. Y. (2012). Polycyclic aromatic hydrocarbons in PM2.5 in Guangzhou, southern China: Spatiotemporal patterns and emission sources. *Journal of Hazardous Materials, 239-240*, 78–87. https://doi.org/10.1016/j.jhazmat.2012.07.068

Gu, Y. G., Li, H. B., & Lu, H. B. (2017). Polycyclic aromatic hydrocarbons (PAHs) in surface sediments from the largest deep plateau lake in China: Occurrence, sources and biological risk. *Ecological Engineering, 101*, 179–184. https://doi.org/10.1016/j.ecoleng.2017.02.007

Han, B., Liu, A., Gong, J., Li, Q., He, X., Zhao, J., & Zheng, L. (2021). Spatial distribution, source analysis, and ecological risk assessment of polycyclic aromatic hydrocarbons (PAHs) in the sediments from rivers emptying into Jiaozhou Bay, China. *Marine Pollution Bulletin, 168*, 112394. https://doi.org/10.1016/j.marpolbul.2021.112394

He, Y., Wang, X., & Zhang, Z. (2023). Polycyclic aromatic hydrocarbons (PAHs) in a sediment core from Lake Taihu and their associations with sedimentary organic matter. *Journal of Environmental Sciences (China), 129*, 79–89. https://doi.org/10.1016/j.jes.2022.09.013

Hong, S., Kim, Y., Lee, Y., Yoon, S. J., Lee, C., Liu, P., Kwon, B., Hu, W., & Khim, J. S. (2022). Distributions and potential sources of traditional and emerging polycyclic aromatic hydrocarbons in sediments from the lower reach of the Yangtze River, China. *Science of The Total Environment, 815*, 152831. https://doi.org/10.1016/j.scitotenv.2021.152831

Hu, G., Luo, X., Li, F., Dai, J., Guo, J., Chen, S., Hong, C., Ma, B., & Xu, M. (2010). Organochlorine compounds and polycyclic aromatic hydrocarbons in surface sediment from Baiyangdian Lake, North China: Concentrations, sources profiles and potential risk. *Journal of Environmental Sciences (China), 22*(2), 176–183. https://doi.org/10.1016/s1001-0742(09)60090-5

Hu, N. J., Huang, P., Liu, J. H., Shi, X. F., Ma, D. Y., & Liu, Y. (2013). Source apportionment of polycyclic aromatic hydrocarbons in surface sediments of the Bohai Sea, China. *Environmental Science and Pollution Research International, 20*(2), 1031–1040. https://doi.org/10.1007/s11356-012-1098-3

Huang, R., Liu, Q., Zhao, Y., Shi, W., & Xu, M. (2021). Pollution status of polycyclic aromatic hydrocarbons in surface sediments off the Jiangsu coastal zone, East China: A case study of Rudong. *Marine Pollution Bulletin, 166*, 112253. https://doi.org/10.1016/j.marpolbul.2021.112253

Huang, T., Zhou, J., Luo, D., Li, S., Yang, H., Huang, C., Li, Y., & Zhang, Z. (2023). Sediment record in pollution, toxicity risk, and source assignment of polycyclic aromatic hydrocarbons (PAHs) in Erhai Lake, Southwest China. *Marine Pollution Bulletin, 186*, 114424. https://doi.org/10.1016/j.marpolbul.2022.114424

Ihunwo, O. C., Ibezim-Ezeani, M. U., & DelValls, T. A. (2021). Human health and ecological risk of polycyclic aromatic hydrocarbons (PAHs) in sediment of Woji creek in the Niger Delta region of Nigeria. *Marine Pollution Bulletin, 162*, 111903. https://doi.org/10.1016/j.marpolbul.2020.111903

Iwegbue, C. M. A., Irerhievwie, G. O., Tesi, G. O., Olisah, C., Nwajei, G. E., & Martincigh, B. S. (2021). Polycyclic aromatic hydrocarbons (PAHs) in surficial sediments from selected rivers in the western Niger Delta of Nigeria: Spatial distribution, sources, and ecological and human health risks. *Marine Pollution Bulletin, 167*, 112351. https://doi.org/10.1016/j.marpolbul.2021.112351

Ji, Z., Zhang, H., Zhang, Y., Chen, T., Long, Z., Li, M., & Pei, Y. (2019). Distribution, ecological risk and source identification of heavy metals in sediments from the Baiyangdian Lake, Northern China. *Chemosphere, 237*, 124425. https://doi.org/10.1016/j.chemosphere.2019.124425

Kalf, D. F., Crommentuiju, T., & Van de Plassche, E. J. (1996). Environmental quality objectives for 10 polycyclic aromatic hydrocarbons (PAHs). *Ecotoxicology and Environmental Safety, 36*, 89–97. https://doi.org/10.1006/eesa.1996.1495

Kanzari, F., Syakti, A. D., Asia, L., Malleret, L., Piram, A., Mille, G., & Doumenq, P. (2014). Distributions and sources of persistent organic pollutants (aliphatic hydrocarbons, PAHs, PCBs and pesticides) in surface sediments of an industrialized urban river (Huveaune), France. *Science of The Total Environment, 478*, 141–151. https://doi.org/10.1016/j.scitotenv.2014.01.065

Li, H., Lai, Z., Zeng, Y., Gao, Y., Yang, W., Mai, Y., & Wang, C. (2021). Occurrence, source identification, and ecological risk assessment of polycyclic aromatic hydrocarbons in sediments of the Pearl River Delta, China. *Marine Pollution Bulletin, 170*, 112666. https://doi.org/10.1016/j.marpolbul.2021.112666

Li, J., Dong, H., Zhang, D., Han, B., Zhu, C., Liu, S., Liu, X., Ma, Q., & Li, X. (2015). Sources and ecological risk

assessment of PAHs in surface sediments from Bohai Sea and northern part of the Yellow Sea, China. *Marine Pollution Bulletin, 96*(1-2), 485–490. https://doi.org/10.1016/j.marpolbul.2015.05.002

Li, J., Yuan, G. L., Li, P., Sun, Y., Yu, H. H., & Wang, G. H. (2017). The emerging source of polycyclic aromatic hydrocarbons from mining in the Tibetan Plateau: Distributions and contributions in background soils. *Science of The Total Environment, 584-585*, 64–71. https://doi.org/10.1016/j.scitotenv.2017.01.146

Li, W., Chen, D., Ruan, W., Peng, Y., Lu, Z., & Wang, D. (2022). Association of polycyclic aromatic hydrocarbons exposure, systemic inflammation with hearing loss among adults and adolescents. *Environmental Pollution, 296*, 118772. https://doi.org/10.1016/j.envpol.2021.118772

Lin, F., Han, B., Ding, Y., Li, Q., Gao, W., & Zheng, L. (2018). Distribution characteristics, sources, and ecological risk assessment of polycyclic aromatic hydrocarbons in sediments from the Qinhuangdao coastal wetland, China. *Marine Pollution Bulletin, 127*, 788–793. https://doi.org/10.1016/j.marpolbul.2017.09.054

Liu, J., Zhao, X., Liu, Y., Qiao, X., Wang, X., Ma, M., Jin, X., Liu, C., Zheng, B., Shen, J., & Guo, R. (2019). High contamination, bioaccumulation and risk assessment of perfluoroalkyl substances in multiple environmental media at the Baiyangdian Lake. *Ecotoxicology and Environmental Safety, 182*, 109454. https://doi.org/10.1016/j.ecoenv.2019.109454

Liu, X., Chen, Z., Xia, C., Wu, J., & Ding, Y. (2020). Characteristics, distribution, source and ecological risk of polycyclic aromatic hydrocarbons (PAHs) in sediments along the Yangtze River Estuary Deepwater Channel. *Marine Pollution Bulletin, 150*, 110765. https://doi.org/10.1016/j.marpolbul.2019.110765

Lu, M., Zeng, D. C., Liao, Y., & Tong, B. (2012). Distribution and characterization of organochlorine pesticides and polycyclic aromatic hydrocarbons in surface sediment from Poyang Lake, China. *Science of The Total Environment, 433*, 491–497. https://doi.org/10.1016/j.scitotenv.2012.06.108

Ma, X., Wan, H., Zhou, J., Luo, D., Huang, T., Yang, H., & Huang, C. (2020). Sediment record of polycyclic aromatic hydrocarbons in Dianchi lake, southwest China: Influence of energy structure changes and economic development. *Chemosphere, 248*, 126015. https://doi.org/10.1016/j.chemosphere.2020.126015

Macdonald, D. D., Scott Carr, R., Calder, F. D., Long, E. R., & Ingersoll, C. G. (1996). Development and evaluation of sediment quality guidelines for Florida coastal waters. *Ecotoxicology, 5*, 253–278. https://doi.org/10.1007/BF00118995

Masood, N., Halimoon, N., Aris, A. Z., Zakaria, M. P., Vaezzadeh, V., Magam, S. M., Mustafa, S., Ali, M. M., Keshavarzifard, M., Alkhadher, S., Bong, C. W., & Alsalahi, M. A. (2018). Seasonal variability of anthropogenic indices of PAHs in sediment from the Kuala Selangor River, west coast Peninsular Malaysia. *Environmental Geochemistry and Health, 40*(6), 2551–2572. https://doi.org/10.1007/s10653-018-0122-z

Mekonnen, K. N., Chandravanshi, B. S., Redi-Abshiro, M., Ambushe, A. A., McCrindle, R. I., & Moyo, S. (2015). Distribution of polycyclic aromatic hydrocarbons in sediments of Akaki River, Lake Awassa, and Lake Ziway, Ethiopia. *Environmental Monitoring and Assessment, 187*(7), 474. https://doi.org/10.1007/s10661-015-4669-1

Montuori, P., Aurino, S., Garzonio, F., Sarnacchiaro, P., Nardone, A., & Triassi, M. (2016). Distribution, sources and ecological risk assessment of polycyclic aromatic hydrocarbons in water and sediments from Tiber River and estuary, Italy. *Science of The Total Environment, 566-567*, 1254–1267. https://doi.org/10.1016/j.scitotenv.2016.05.183

Riaz, R., Ali, U., Li, J., Zhang, G., Alam, K., Sweetman, A. J., Jones, K. C., & Malik, R. N. (2019). Assessing the level and sources of polycyclic aromatic hydrocarbons (PAHs) in soil and sediments along Jhelum riverine system of lesser Himalayan region of Pakistan. *Chemosphere, 216*, 640–652. https://doi.org/10.1016/j.chemosphere.2018.10.139

Rodrigues, F., Martins, D. A., Morais, P. V., Oliveira, A. H. B., Gama, A. F., Nascimento, R. F., Choi-Lima, K. F., Moreira, L. B., Abessa, D. M. S., Nelson, R. K., Reddy, C. M., Swarthout, R. F., & Cavalcante, R. M. (2019). Influence of anthropogenic activities and risk assessment on protected mangrove forest using traditional and emerging molecular markers (Ceará coast, northeastern Brazil). *Science of the Total Environment, 656*, 877–888. https://doi.org/10.1016/j.scitotenv.2018.11.380

Shi, C., Qu, C., Sun, W., Zhou, J., Zhang, J., Cao, Y., Zhang, Y., Guo, J., Zhang, J., & Qi, S. (2022a). Multimedia distribution of polycyclic aromatic hydrocarbons in the Wang Lake Wetland, China. *Environmental Pollution, 306*, 119358. https://doi.org/10.1016/j.envpol.2022.119358

Shi, W., Gong, H., Zhou, W., Tan, X., Zhang, C., & Dai, X. (2023). Distribution and ecological risk of polycyclic aromatic hydrocarbons in wastewater treatment plant sludge and sewer sediment from cities in Middle and Lower Yangtze River. *Science of The Total Environment, 881*, 163212. https://doi.org/10.1016/j.scitotenv.2023.163212

Shi, W., Xu, M., Liu, Q., & Xie, S. (2022b). Polycyclic aromatic hydrocarbons in seawater, surface sediment, and marine organisms of Haizhou Bay in Yellow Sea, China: Distribution, source apportionment, and health risk assessment. *Marine Pollution Bulletin, 174*, 113280. https://doi.org/10.1016/j.marpolbul.2021.113280

Singare, P. U. (2015). Studies on polycyclic aromatic hydrocarbons in surface sediments of Mithi River near Mumbai, India: Assessment of sources, toxicity risk and biological impact. *Marine Pollution Bulletin, 101*(1), 232–242. https://doi.org/10.1016/j.marpolbul.2015.09.057

Škrbić, B. D., Kadokami, K., & Antic, I. (2018). Survey on the micro-pollutants presence in surface water system of northern Serbia and environmental and health risk assessment. *Environmental Research, 166*, 130–140. https://doi.org/10.1016/j.envres.2018.05.034

Sofowote, U. M., McCarry, B. E., & Marvin, C. H. (2008). Source apportionment of PAH in Hamilton Harbour suspended sediments: Comparison of two factor analysis methods. *Environmental Science & Technology, 42*, 6007–6014. https://doi.org/10.1021/es800219z

Sun, T., Wang, Y., Chen, Y., Zhang, M., & Kong, X. (2022). Occurrence of polycyclic aromatic hydrocarbons in the estuarine sediments of the Taihu Lake and their associated toxic effects on aquatic organisms. *Pedosphere, 32*(6), 833–843. https://doi.org/10.1016/j.pedsph.2022.06.021

Wang, S., Tang, C., Song, X., Wang, Q., Zhang, Y., & Yuan, R. (2014). The impacts of a linear wastewater reservoir on groundwater recharge and geochemical evolution in a semi-arid area of the Lake Baiyangdian watershed, North China Plain. *Science of The Total Environment, 482-483*, 325–335. https://doi.org/10.1016/j.scitotenv.2014.02.130

Wang, J., Zeng, X., Xu, D., Gao, L., Li, Y., & Gao, B. (2020). Chemical fractions, diffusion flux and risk assessment of potentially toxic elements in sediments of Baiyangdian Lake, China. *Science of The Total Environment, 724*, 138046. https://doi.org/10.1016/j.scitotenv.2020.138046

Wang, Y. S., Wu, F. X., Gu, Y. G., Huang, H. H., Gong, X. Y., & Liao, X. L. (2021). Polycyclic aromatic hydrocarbons (PAHs) in the intertidal sediments of Pearl River Estuary: Characterization, source diagnostics, and ecological risk assessment. *Marine Pollution Bulletin, 17*, 113140. https://doi.org/10.1016/j.marpolbul.2021.113140

Wu, Q., He, B., Guo, R., Cui, J., Yan, S., Liu, D., & Yao, B. (2021). Fluorescent whitening agents in Baiyangdian Lake in North China: Analysis, occurrence, distribution and ecological risk assessment. *Environmental Pollution, 291*, 118235. https://doi.org/10.1016/j.envpol.2021.118235

Yang, L., Wang, T., Zhou, Y., Shi, B., Bi, R., & Meng, J. (2021). Contamination, source and potential risks of pharmaceuticals and personal products (PPCPs) in Baiyangdian Basin, an intensive human intervention area, China. *Science of The Total Environment, 760*, 144080. https://doi.org/10.1016/j.scitotenv.2020.144080

Zhang, L., Shen, L., Qin, S., Cui, J., & Liu, Y. (2020). Quinolones antibiotics in the Baiyangdian Lake, China: Occurrence, distribution, predicted no-effect contents (PNECs) and ecological risks by three methods. *Environmental Pollution, 256*, 113458. https://doi.org/10.1016/j.envpol.2019.113458

Zhang, Q., Meng, J., Su, G., Liu, Z., Shi, B., & Wang, T. (2021). Source apportionment and risk assessment for polycyclic aromatic hydrocarbons in soils at a typical coking plant. *Ecotoxicology and Environmental Safety, 222*, 112509. https://doi.org/10.1016/j.ecoenv.2021.112509

Zhang, Z., Li, J., Li, Y., Zhao, L., & Duan, X. (2022). Accumulation of polycyclic aromatic hydrocarbons in the road green infrastructures of sponge city in Northwestern China: Distribution, risk assessments and microbial community impacts. *Journal of Cleaner Production, 350*, 131494. https://doi.org/10.1016/j.jclepro.2022.131494

Zhao, Y., Han, J., Zhang, B., & Gong, J. (2021). Impact of transferred water on the hydrochemistry and water quality of surface water and groundwater in Baiyangdian Lake, North China. *Geoscience Frontiers, 12*(3), 101086. https://doi.org/10.1016/j.gsf.2020.09.015

Zheng, H., Yang, D., Hu, T., Li, Y., Zhu, G., Xing, X., & Qi, S. (2017). Source apportionment of polycyclic aromatic carbons (PAHs) in sediment core from Honghu Lake, central China: Comparison study of three receptor models. *Environmental Science and Pollution Research International, 24*(33), 25899–25911. https://doi.org/10.1007/s11356-017-0185-x

Zhou, Z., Zhang, P., Zhang, G., Wang, S., Cai, Y., & Wang, H. (2021). Vertical microplastic distribution in sediments of Fuhe River estuary to Baiyangdian Wetland in Northern China. *Chemosphere, 280*, 130800. https://doi.org/10.1016/j.chemosphere.2021.130800